

Journal of Visualized Experiments

Surgery and Sample Processing for Correlative Imaging of the Murine Pulmonary Valve

--Manuscript Draft--

Article Type:	Methods Article - JoVE Produced Video
Manuscript Number:	JoVE62581R2
Full Title:	Surgery and Sample Processing for Correlative Imaging of the Murine Pulmonary Valve
Corresponding Author:	Felix Liu, Ph.D The Ohio State University Columbus, Ohio UNITED STATES
Corresponding Author's Institution:	The Ohio State University
Corresponding Author E-Mail:	liu.612@osu.edu
Order of Authors:	Yifei Liu, Ph.D Yong-Ung Lee Tai Yi Ken Wu Cedric Bouchet-Marquis Han Chan Christopher Breuer David McComb
Additional Information:	
Question	Response
Please indicate whether this article will be Standard Access or Open Access.	Standard Access (US\$2,400)
Please specify the section of the submitted manuscript.	Engineering
Please indicate the city, state/province, and country where this article will be filmed . Please do not use abbreviations.	Columbus, Ohio, USA
Please confirm that you have read and agree to the terms and conditions of the author license agreement that applies below:	I agree to the Author License Agreement
Please provide any comments to the journal here.	
Please indicate whether this article will be Standard Access or Open Access.	Standard Access (\$1400)

TITLE:

Surgery and Sample Processing for Correlative Imaging of the Murine Pulmonary Valve

AUTHORS AND AFFILIATIONS:

Yifei Liu¹, Yong-Ung Lee², Tai Yi², Ken Wu³, Cedric Bouchet-Marquis³, Han Chan³, Christopher K. Breuer^{1,2}, David W. McComb¹

¹Center for Electron Microscopy and Analysis, The Department of Materials Science and Engineering, Ohio State University, Columbus, OH, United States

²Center for Regenerative Medicine, Nationwide Children's Hospital, Columbus, OH, United States

³Thermo Fisher Scientific, Hillsboro, OR, United States

E-mail addresses of co-authors:

Yifei Liu	(liu.612@osu.edu)
Yong-Ung Lee	(yongung.lee@gmail.com)
Tai Yi	(tai.yi@nationwidechildrens.org)
Ken Wu	(ken.wu@thermofisher.com)
Cedric Bouchet-Marquis	(cedric.bouchet-marquis@thermofisher.com)
Han Chan	(han.chan@thermofisher.com)
Christopher K. Breuer	(christopher.breuer@nationwidechildrens.org)
David W. McComb	(mccomb.29@osu.edu)

E-mail addresses of corresponding authors:

Yifei Liu	(liu.612@osu.edu)
-----------	-------------------

KEYWORDS:

murine pulmonary valve, heart valve, collagen, extracellular matrix, correlative imaging, serial block face scanning electron microscopy, micro-computed tomography, heart valve disease

SUMMARY:

Here, we describe a correlative workflow for the excision, pressurization, fixation, and imaging of the murine pulmonary valve to determine the gross conformation and local extracellular matrix structures.

ABSTRACT:

The underlying causes of the heart valve related disease (HVD) are elusive. Murine animal models provide an excellent tool for studying HVD, however, the surgical and instrumental expertise required to accurately quantify the structure and organization across multiple length scales have stunted its advancement. This work provides a detailed description of the murine dissection, en bloc staining, sample processing, and correlative imaging procedures for depicting the heart valve at different length scales. Hydrostatic transvalvular pressure was used to control the temporal heterogeneity by chemically fixing the heart valve conformation. Micro-computed tomography (μ CT) was used to confirm the geometry of the heart valve and provide a reference for the downstream sample processing needed for the serial block face scanning electron microscopy

(SBF-SEM). High-resolution serial SEM images of the extracellular matrix (ECM) were taken and reconstructed to provide a local 3D representation of its organization. μ CT and SBF-SEM imaging methods were then correlated to overcome the spatial variation across the pulmonary valve. Though the work presented is exclusively on the pulmonary valve, this methodology could be adopted for describing the hierarchical organization in biological systems and is pivotal for the structural characterization across multiple length scales.

INTRODUCTION:

The pulmonary valve (PV) serves to ensure unidirectional blood flow between the right ventricle and the pulmonary artery. Pulmonary valve malformations are associated with several forms of congenital heart disease. The current treatment for congenital heart valve disease (HVD) is valvular repair or valve replacement, which can necessitate multiple invasive surgeries throughout a patient's lifetime¹. It has been widely accepted that the function of the heart valve is derived from its structure, often referred to as the structure-function correlate. More specifically, the geometric and biomechanical properties of the heart dictate its function. The mechanical properties, in turn, are determined by the composition and organization of the ECM. By developing a method for determining the biomechanical properties of murine heart valves, transgenic animal models can be used to interrogate the role of the ECM on heart valve function and dysfunction²⁻⁵.

The murine animal model has long been regarded as the standard for molecular studies because transgenic models are more readily available in mice compared to other species. Murine transgenic models provide a versatile platform for researching heart valve related diseases⁶. However, the surgical expertise and instrumentation requirements to characterize both the geometry and ECM organization have been a major hurdle in progressing HVD research. Histological data in literature provides a picture of the content of the murine heart valve extracellular matrix, but only in the form of 2D images, and are unable to describe its 3D architecture^{7,8}. Additionally, the heart valve is both spatially and temporally heterogeneous, making it difficult to draw conclusions across experiments regarding ECM organization if the sampling and conformation are not fixed. Conventional 3D characterization methods, such as MRI or 3D echocardiography, do not provide the resolution necessary to resolve ECM components^{9,10}.

This work details a fully correlative workflow where the temporal heterogeneity due to the cardiac cycle was addressed by fixing the conformation of the murine PV with hydrostatic transvalvular pressure. The spatial heterogeneity was controlled precisely by sampling regions of interest and registering data sets from different imaging modalities, specifically μ CT and serial block face scanning electron microscopy, across different length scales. This method of scouting with μ CT for guiding downstream sampling has been proposed previously, but because the pulmonary valve exhibits temporal variation, an additional level of control was needed on the surgical level¹¹.

In vivo studies describing murine heart valve biomechanics are sparse and, instead, rely on computational models when describing the deformation behavior. It is of critical importance that

local extracellular data on the nanometer length scale be related to the geometry and location of the heart valve. This, in turn, provides quantifiable, spatially mapped distributions of mechanically contributing ECM proteins, which can be used to reinforce existing biomechanical heart valve models¹²⁻¹⁴.

PROTOCOL:

The use of animals in this study was in accordance with Nationwide Children's Hospital institutional animal care and use committee under protocol AR13-00030.

1. Pulmonary valve excision

1.1. Autoclave the necessary tools needed for the mouse dissection. This includes fine scissors, micro forceps, micro vascular clamps, clamp applying forceps, microneedle holders, spring scissors, and retractors.

1.2. Acclimate all mice for a minimum of 2 weeks before the operation. Remove C57BL/6 mice, approximately 1 year of age, from their cages and weigh, then euthanize with a ketamine/xylazine cocktail (3:1 ketamine:xylazine, 0.01 mL per g) overdose.

1.3. Place the mouse in a dorsal recumbence position on a tray and secure its limbs with tape. Once secured, perform the thoracotomy.

1.3.1. Expose the heart by removing any excess adipose tissue and fascia.

1.3.2. Remove the right atrium and perfuse through the left ventricle with room temperature saline solution (0.9% NaCl). The perfusion should take approximately 20 mL over 30 s. This results in the exsanguination of the mouse.

1.4. Remove the entire heart by severing the superior vena cava, inferior vena cava, pulmonary artery, and aorta. Special care should be taken for the pulmonary artery. Cut approximately 2 mm above the ventriculo-arterial junction, as this will serve as the conduit for pressurization.

1.5. Remove the left and right ventricles to expose chambers to atmospheric pressure. Ensure that the structure of the pulmonary trunk should be unaffected by the removal of the ventricles.

2. Pressure fixation of pulmonary valve

2.1. Anastomose pressurization tubing with pulmonary artery, leaving approximately 1 mm distance between the sino-tubular junction and the end of the tubing to accommodate for large movements of the leaflets and pulmonary trunk.

2.2. Elevate the reservoir to an analogous physiological pressure and fill it with the saline solution. Test the flow-through system to ensure there are no blockages or air bubbles.

2.3. Attach a stopcock to the anastomosed pulmonary valve and ensure adequate flow through the tubing (i.e., no air bubbles) by switching the outflow tract. Once the flow is adequate, switch the outflow to the anastomosed pulmonary valve and ensure pressurization of the pulmonary trunk. This is identified by pulmonary trunk distention.

2.4. Once the pressurization of the pulmonary trunk is confirmed, gradually incorporate primary fixative solution (1.25% glutaraldehyde, 1.0% paraformaldehyde in 0.15 M cacodylate) until the saline solution is purged. This is done by removing a portion, approximately 25% of the reservoir capacity, of the saline solution and replacing it with the primary fixative.

CAUTION: The fixatives used (paraformaldehyde and glutaraldehyde) are highly toxic and appropriate personal protective equipment (PPE) should be worn to ensure safety.

2.5. Place a fixative-soaked gauze over the tissue sample to prevent drying.

2.6. Perfuse the fixative for 3 h, refilling the reservoir as needed to maintain a constant pressure. Throughout fixation, it is not uncommon for the pulmonary valve to shrink because of the chemical fixation. If this is the case, constantly replenish the reservoir with primary fixative to maintain physiological pressure.

2.7. Store the heart valve in the fixative solution at 4 °C until use. Samples were stored for up to 1 week without any discernable difference.

3. En bloc sample staining and embedment^{15,16}

CAUTION: The staining reagents used in this section (potassium ferrocyanide, osmium tetroxide, thiocarbohydrazide, lead aspartate, and uranyl acetate) are highly toxic and should be handled with extreme care. Use of a fume hood and proper PPE is advised.

3.1. Staining

3.1.1. Wash the fixed heart valve sample for 5 min with cold 0.15 M cacodylate buffer. Repeat the wash two more times.

3.1.2. Completely submerge the heart valve in a solution of 1.5% potassium ferrocyanide, 0.15 M cacodylate, 2 mM calcium chloride, and 2% osmium tetroxide, on ice for 1 h.

3.1.3. While the sample is incubating, prepare thiocarbohydrazide (TCH) solution by dissolving 0.1 g of TCH in 10 mL of ddH₂O. Place the solution in a 60 °C oven for 1 h. Gently agitate periodically to ensure TCH is dissolved completely. Filter the solution through a 0.22 µm syringe filter immediately before use.

3.1.4. Wash the samples with room temperature ddH₂O by placing them in a tube of ddH₂O for 5 min and slightly agitate it by shaking the container. Repeat this process three times.

3.1.5. Place it in filtered TCH solution for 20 min at room temperature. Perform the washing step three times (5 min each) with room temperature ddH₂O as described in step 3.1.4.

3.1.6. Once done, place the sample in 2% osmium tetroxide for 30 min at room temperature. Then wash it again for a total of three times for 5 min each with room temperature ddH₂O.

3.1.7. Incubate the sample in 1% uranyl acetate overnight at 4 °C.

3.1.8. During this time, make a solution of 0.066 g of lead nitrate in 10 mL of aspartic acid stock solution. Adjust the pH to 5.5 with 1 N KOH. Place the solution in a 60 °C oven to dissolve lead nitrate.

3.1.9. After the overnight incubation, perform the washing step as described in step 3.1.4. Repeat three times. Then, incubate the heart valve tissue in lead aspartate solution from step 3.1.8 in a 60 °C oven for 30 min.

3.2. Dehydration

3.2.1. Wash the tissues for 5 min at room temperature with ddH₂O. Repeat three times.

3.2.2. Make fresh solutions of 20%, 50%, 70%, 90%, and 100% ethanol in ddH₂O. Keep on ice until use.

3.2.3. To dehydrate the heart valve tissue. Perform subsequent treatments of 20%, 50%, 70%, and 90% ethanol on ice for 5 min each. Then perform two subsequent treatments of 100% ethanol on ice for 5 min.

3.2.4. Move the tissue to ice-cold acetone for 10 min. Then place in fresh acetone at room temperature for 10 min.

3.3. Embedding

3.3.1. Make the resin mixture (see **Table of Materials**) according to the manufacturer's specifications: 11.4 g of component A, 10 g of component B, 0.3 g of component C, and 0.05–0.1 g of component D. Initially mix components A and B by heating each of the components to 60 °C before adding components C and D. The mixture will turn into an amber color upon adding components C and D. It will be uniform when properly mixed.

3.3.2. Make mixtures with volume ratios of 25:75, 50:50, and 75:25 resin:acetone. Mix thoroughly.

3.3.3. Place tissues in subsequent treatments of the 25:75, 50:50, and 75:25 resin:acetone mixture for 2 h each at room temperature.

3.3.4. Place tissues in 100% resin overnight at room temperature.

3.3.5. The following day, place tissues in fresh 100% resin for 2 h at room temperature.

3.3.6. Transfer the heart valve tissues to an embedding capsule, substitute with fresh 100% resin, and place in a 60 °C oven for 48 h to cure.

3.4 Perform correlative imaging as shown below.

4. Micro-computed tomography imaging

4.1. Mount the resin sample block onto a μ CT sample holder with an adhesive (glue or double-sided tape works well).

4.2. Place the holder into μ CT chamber and fix it onto the stage by screwing the collet such that there is no motion of the holder. Sample movement during the scan will decrease the image quality.

4.3. Open the μ CT user interface by double-clicking on the icon. Add a project by selecting the + sign next to **Projects** and fill in the necessary fields.

4.4. Once this is created, find the created project, and select it by clicking on it. This will open up a second column **Acquisitions**. Select the + next to **Acquisitions** and fill out the necessary fields.

4.5. Close the chamber doors and arm the system by hitting the arming button on the front panel or the μ CT. Warmup x-rays from the user interface by selecting the button indicating **Warmup**.

NOTE: The system will automatically turn off the x-rays following a successful warm-up procedure. Turn on x-rays by selecting the button.

4.6. Adjust the stage rotation such that the center of the rotation of the sample does not deviate from the center of the monitor (i.e., the sample is within the field of view for the entire scan). For the system used for this experiment, this involves adjusting the region of interest (ROI) stage under the drop-down tab as detailed below.

4.6.1. Set the ROI stage adjustment by setting the rotation angle to 0° and marking the edge of the sample. The sample is then rotated to 180° and the edge of the sample is marked again.

4.6.2. Adjust the ROI stage x-axis position such that the edge of the sample is between these two extremes. Repeat this process for rotation angles of 90° and 270° for the y-position.

4.6.3. In the case where the rotation of the sample causes the edges to move out of the field of view, decrease the magnification of the μ CT needs until the edges of the sample are visible at the

above set angles and a coarse ROI stage adjustment can be made.

4.6.4. Once adjusted at the lower magnification, move the sample or the detector to increase the magnification and the ROI positions can be fine adjusted.

NOTE: This process may need to be repeated to ensure alignment. Proper alignment results in a sample that shows little to no horizontal movement through all sample rotation angles.

4.7. Adjust the μ CT to desired scanning parameters using the manufacturer's software. These parameters include tube potential, tube current, detector distance, sample distance, exposure time, trajectory, and the number of projections (see **Table S1** for the μ CT acquisition parameters used in this study).

NOTE: Calibration parameters, such as clear field and dark field scans, should be kept at the manufacturer's specifications unless otherwise stated. For example, if a sample is too large and the system cannot move the sample out of the field view, then the sample needs to be removed to perform clear field calibration scans.

4.8. Once the parameters are set, an approximation of the duration of the scan can be seen by hitting the **Time Estimate** button. Select the **Start** button to begin the scan.

4.9. Following the scan completion, ensure that the x-rays are turned off, unscrew the collet, and carefully remove the sample from the μ CT chamber.

5. Sample processing and image correlation

5.1. Reconstruct μ CT projections using a filtered back projection algorithm with the software provided by the manufacturer (see **Table of Materials**).

5.1.1. Select the **Recon** tab at the top of the screen. Select the **Project** and **Acquisition** tab.

5.1.2. Select the recon template associate with filtered back projection. Hit the **Start Recon** button.

5.2. Identify and segment the pulmonary valve using image processing software. This requires prior knowledge of the anatomy of the pulmonary valve¹⁷. At elevated arterial pressures, the leaflets coapt and block the lumen of the pulmonary valve.

5.3. Identify the slicing orientation with respect to the scanning direction and sample. Reorient the sample such that the slicing direction is aligned with the desired axis.

5.4. Identify regions of interest for high-resolution imaging. In this experiment, the belly (middle) of the leaflet and the arterio-valvular junction was chosen.

5.5. Remove the excess resin and sample by either razor blade or sanding for large pieces of material, or by microtome for finer pieces.

5.6. Once at a location of interest, compare the physical specimen with virtual μ CT slices to confirm location. This was done by comparing anatomical features at the cross section.

6. Serial block face scanning electron microscopy¹⁸

6.1. Reduce the cross-section of the specimen to accommodate SBF-SEM, approximately 2.0 x 1.5 x 1.8 mm.

6.2. Mount the trimmed sample onto the SBF-SEM aluminum stub using epoxy.

6.3. Coat the specimen block with 35 nm gold. Spin the sample on the platform to apply an even layer of coating.

6.4. Vent the SBF-SEM chamber and adjust the height of the knife blade to microscope eucentric height.

6.5. Insert the sample and level the sample stub.

6.6. Image under low vacuum conditions to prevent charging and with backscatter detector (see **Table S2** for SBF-SEM acquisition parameters).

6.7. Image and stitch multiple regions of interest at different magnifications using automated software (see **Table of Materials**).

REPRESENTATIVE RESULTS:

Anastomosis of the pulmonary artery to the pressurization tubing is shown in **Figure 1A**. Following the application of hydrostatic pressure, the pulmonary trunk distends radially (**Figure 1B**) indicating that the pulmonary valve leaflets are in a closed configuration. Pulmonary valve conformation was confirmed by μ CT. In this case, the leaflets were coapt (closed) and the annulus was circular (**Figure 2A**). **Figure 2B,C** shows varying degrees of inadequate pulmonary valve pressurization by either fixation (**Figure 2B**) or arterial collapse (**Figure 2C**).

Sample block trimming was guided by the μ CT volume rendering. In this case, the plane parallel to the sino-tubular junction was chosen as the slicing direction. Using anatomical landmarks, the μ CT volume rendering virtual cross sections was correlated with optical images (**Figure 3**) to confirm the slicing direction and location.

Once the specimen block was at the desired location and orientation, high-resolution SBF-SEM images were taken at a local region within a leaflet. Image correlation was done between the μ CT volume rendering virtual slice (**Figure 4A**), low-resolution SBF-SEM images (**Figure 4B**), and high-resolution SBF-SEM images (**Figure 4C**). Because of the manual sample mounting, requisite

slices of the specimen block were needed to create a flat surface before acquiring images in the SBF-SEM; hence, the different locations between **Figure 3** and **Figure 4**.

A full image correlation between μ CT and SBF-SEM data sets can be seen in **Video 1**. The pulmonary valve specimen in the μ CT volume rendering can be easily discerned from the surrounding embedding resin because of the staining of heavy metal atoms. Lengths and angles are measured in the image to guide the slicing. In this example, the plane parallel to the sinotubular junction was used. A virtual slice through emulates the removal of the material until the depth of interest is reached. High-resolution images taken by SBF-SEM were taken at this cross section and registered to the μ CT data set.

Once acquired, high-resolution images taken by SBF-SEM can be imported into an image processor and compiled into a 3D representation (**Figure 5**) where extracellular components can be identified.

FIGURE AND TABLE LEGENDS:

Figure 1: Representative images of anastomosed pulmonary trunk. The excised pulmonary trunk (**A**) before and (**B**) after hydrostatic pressurization. The dotted line indicates the ventriculoarterial junction where the annulus of the pulmonary trunk resides. Note the pulmonary trunk distention upon pressurization.

Figure 2: Representative μ CT volume rendering pulmonary valve. (**A**) The pulmonary valve is in a closed position with the leaflets adequately stretched and coapt (circle). (**B,C**) Inadequate pressurization of the pulmonary valve. Note that the leaflets are not properly coapt (**B**) and that the annulus is not circular (**C**).

Figure 3: Image correlation of pulmonary valve specimen block. (**A**) μ CT volume rendering virtual slice and (**B**) physical specimen block after trimming taken by optical microscopy. Sections of pulmonary valve leaflets are circled in red and were used as landmarks to correlate the two different imaging methods. Scale bar corresponds to 500 μ m.

Figure 4: Image correlation of imaged pulmonary valve cross section. (**A**) Virtual cross section generated by μ CT volume rendering. Red box indicates the region that was imaged using SBF-SEM in (**B**). (**B**) Low-resolution overview images to correlate with μ CT cross section. Blue box represents the location of (**C**) high-resolution SBF-SEM imaging. Scale bars correspond to (**B**) 100 μ m and (**C**) 10 μ m.

Figure 5: Segmented region of the pulmonary valve taken by SBF-SEM. Cross-sectional images were stacked and compiled to form a 3D representation of a local pulmonary valve region. Labels were assigned to endothelial cells (green), valvular interstitial cells (blue), and extracellular fibers (yellow). The approximate dimensions of the imaged region are 30 μ m x 20 μ m x 100 μ m.

Table S1: Imaging parameters for μ CT.

Table S2: Imaging parameters for SBF-SEM.

Video 1: Image correction of μ CT and SBF-SEM data sets.

DISCUSSION:

Removal of the ventricles serves two purposes. First, exposing the ventricle side to the atmospheric pressure, thereby only needing to apply a transvalvular pressure from the arterial side of the pulmonary valve to close, and second, providing a stable base to prevent twisting of the pulmonary trunk. During pressurization, the pulmonary trunk distends radially and inferiorly, making it prone to twisting, causing the collapse of the pulmonary trunk. Preloading the pulmonary valve with a saline solution offers an additional quality check to ensure that the pressurization is adequate and if there are any leaks in the system. The action of the primary fixative is quick, in the order of a few seconds, and without hydrostatic preloading with the saline solution, the pulmonary valve is fixed in a random conformation. Without preloading, the success rate for a closed pulmonary valve was around 10%–20%. With the preloading step, the success rate was above 90%.

The μ CT and SBF-SEM imaging conditions were tuned for this application. The pulmonary valve, when fully stretched, can be less than 10 μ m thick. As a rule of thumb, a threshold of 3 voxels is required for being able to resolve a feature; so the μ CT volume renderings were scanned with a voxel size of 2.9 μ m with a field of view of 8.4 x 8.4 x 6.3 mm. Smaller voxel sizes can be achieved in μ CT but this requires either sample trimming and/or longer scan times. A smaller sample would allow higher resolution by placing it closer to the x-ray source. Smaller voxels can also be achieved by placing the x-ray detector further back from the sample; however, this will decrease the total flux on the detector and compromise the signal-to-noise ratio. As a reference, our μ CT scans were approximately 5–6 h in duration. Specific imaging conditions used in this study are in the **Supplementary Tables S1 and Supplementary Tables S2**).

There are limitations to this method. The surgical portion of this procedure requires expertise in animal handling to not compromise the pulmonary valve structure while handling. Additionally, the imaging is time-intensive and requires multiple imaging instruments. As a reference, the high-resolution SBF-SEM imaging was approximately 1 week of the continuous imaging for a depth of around 100 μ m. This is a demanding task for the instrument to remain stable and consistent for long imaging sessions. A more practical approach would be to devise a sampling strategy to precisely portray the heterogeneity of the pulmonary valve without the time investment. This is yet to be determined. To date, the entire correlative workflow has been done on one mouse but has shown the feasibility and potential of the correlative workflow in investigating the pulmonary valve across length scales.

Future iterations of this correlative approach may involve *in situ* μ CT experiments, such that the same sample can be exposed to different transvalvular pressure to remove sample-to-sample variation. This is currently limited by sample and instrument stability for extended scan times, a pressurization apparatus integrated into imaging systems, and contrast due to similar

attenuation coefficient of water and tissue. Additionally, though the transvalvular pressures were reflective of physiological conditions, it is not representative of the pulsatile flow that is characteristic of cardiac contraction. However, it has been shown that strain rate has little effect on the conformation of the leaflet. In future iterations, it might prove more relevant to engineer a device capable of administering pulsatile flow⁹. Additionally, much of the work requires manual interrogation of the sample, as currently there is no automated workflow. Locating the pulmonary valve, sample processing toward the region of interest, image correlation, and registration were done manually, but would prove useful in the future to streamline processing and mitigate subjectivity.

The work presented is a correlative workflow for fixing the conformation of the pulmonary valve and registering imaging in μ CT and SBF-SEM. The information obtained using this method will ultimately be utilized to determine the underlying biomechanics of the pulmonary valve in murine animal models, which have yet to be elucidated. Valvular biomechanics can be completely described by its geometry and extracellular matrix, but these are on two different length scales. To do this, precise control of the heterogeneity of the valve and accurate mapping of high-resolution images of the extracellular matrix with respect to its location within the pulmonary valve is needed. This correlative workflow is already being implemented into other experiments to draw comparisons between wild-type and transgenic osteogenesis imperfecta mice to compare fibrillar extracellular matrix differences and can readily be extrapolated to other congenital defects such as bicuspid valve formation^{19,20}. This information coupled with possible proteomics will provide a complete picture of how the biomechanics will differ between the two murine animal models.

Despite this work only portraying the pulmonary valve, this workflow is readily amendable to other heterogeneous, hierarchical biological systems. We utilized 3D imaging techniques to capture the architectural organization of the ECM, but higher resolution techniques, such as transmission electron microscopy or scanning transmission electron microscopy, can be appended depending on the information desired.

ACKNOWLEDGMENTS:

This work is supported, in part, by R01HL139796 and R01HL128847 grants to CKB and RO1DE028297 and CBET1608058 for DWM.

DISCLOSURES:

The authors have nothing to disclose.

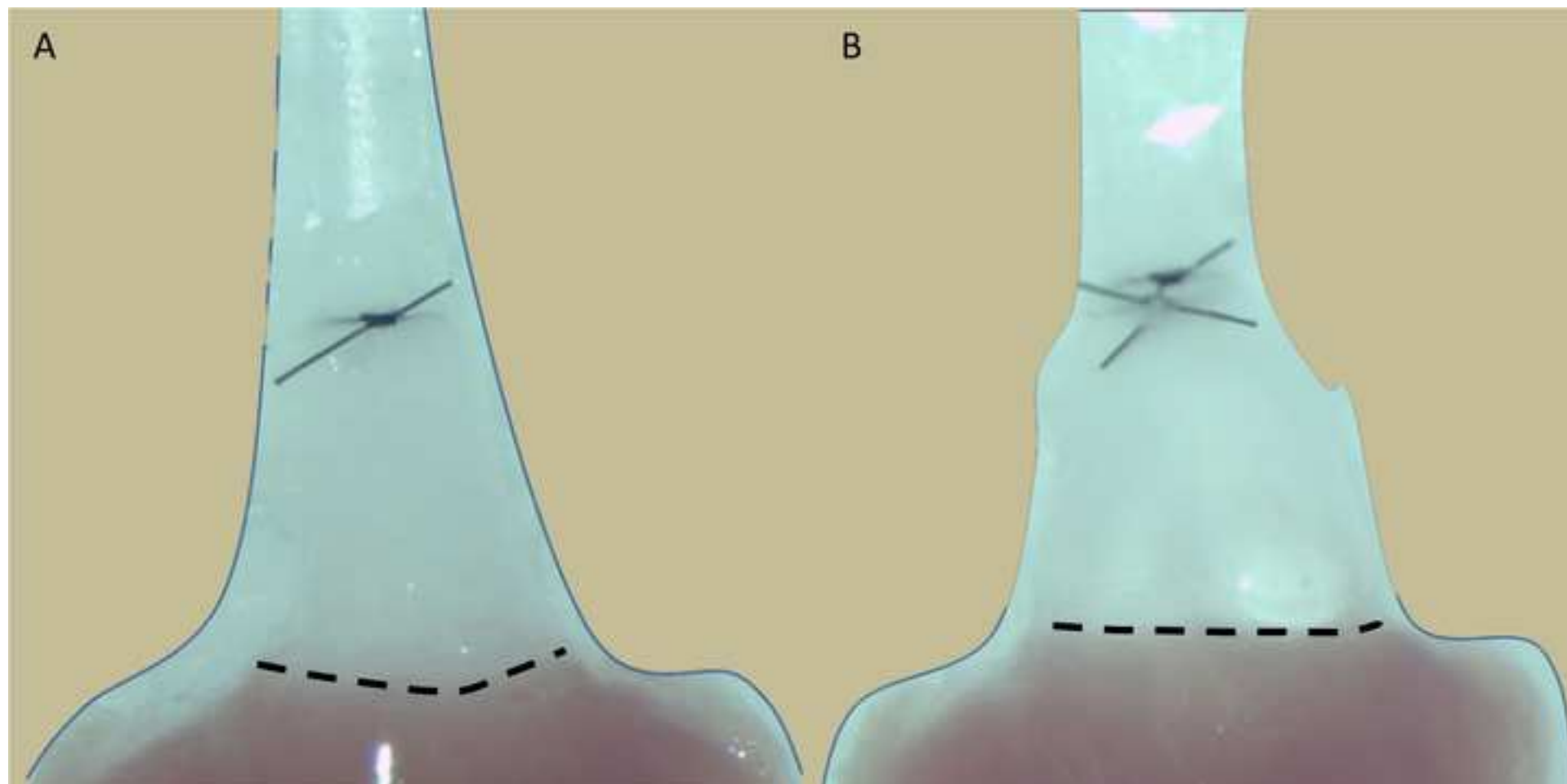
REFERENCES:

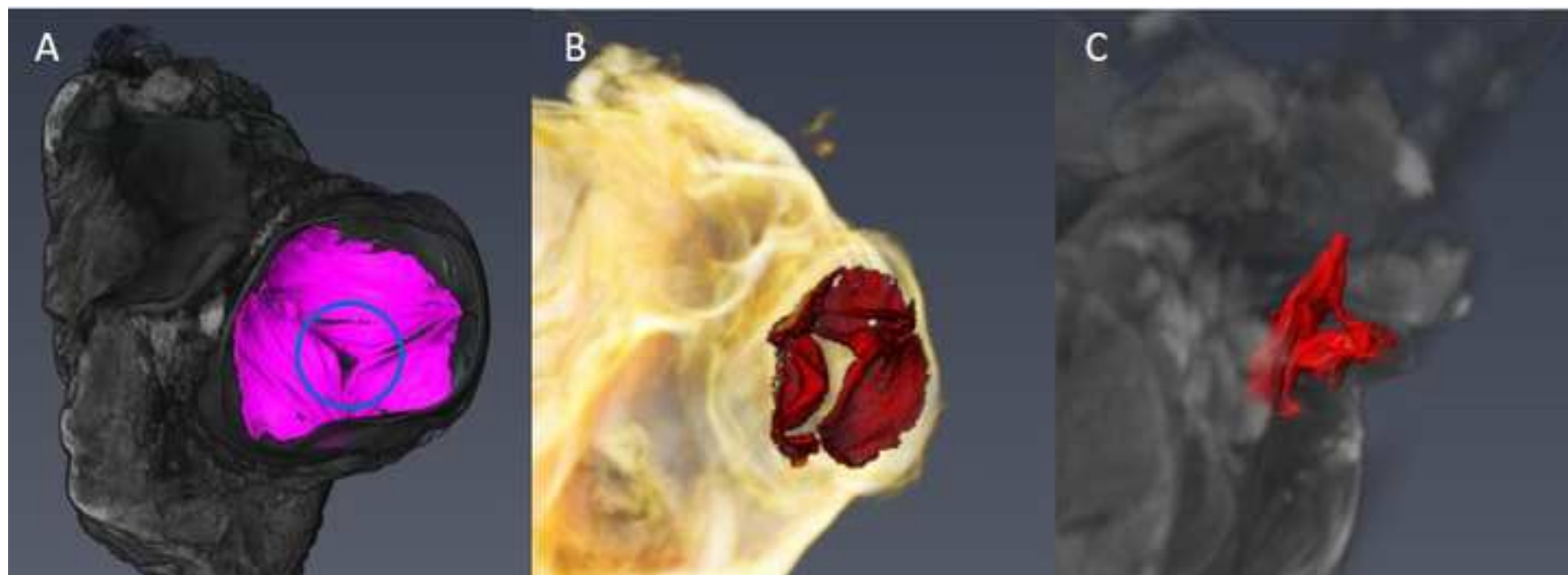
1. Azari, S. et al. A systematic review of the cost-effectiveness of heart valve replacement with a mechanical versus biological prosthesis in patients with heart valvular disease. *Heart Failure Reviews*. **25** (3), 495–503 (2020).
2. Ng, C.M. et al. TGF- β –dependent pathogenesis of mitral valve prolapse in a mouse model of Marfan syndrome. *Journal of Clinical Investigation*. **114** (11), 1586–1592 (2004).
3. Cheek, J. D., Wirrig, E. E., Alfieri, C. M., James, J. F., Yutzey, K. E. Differential activation of

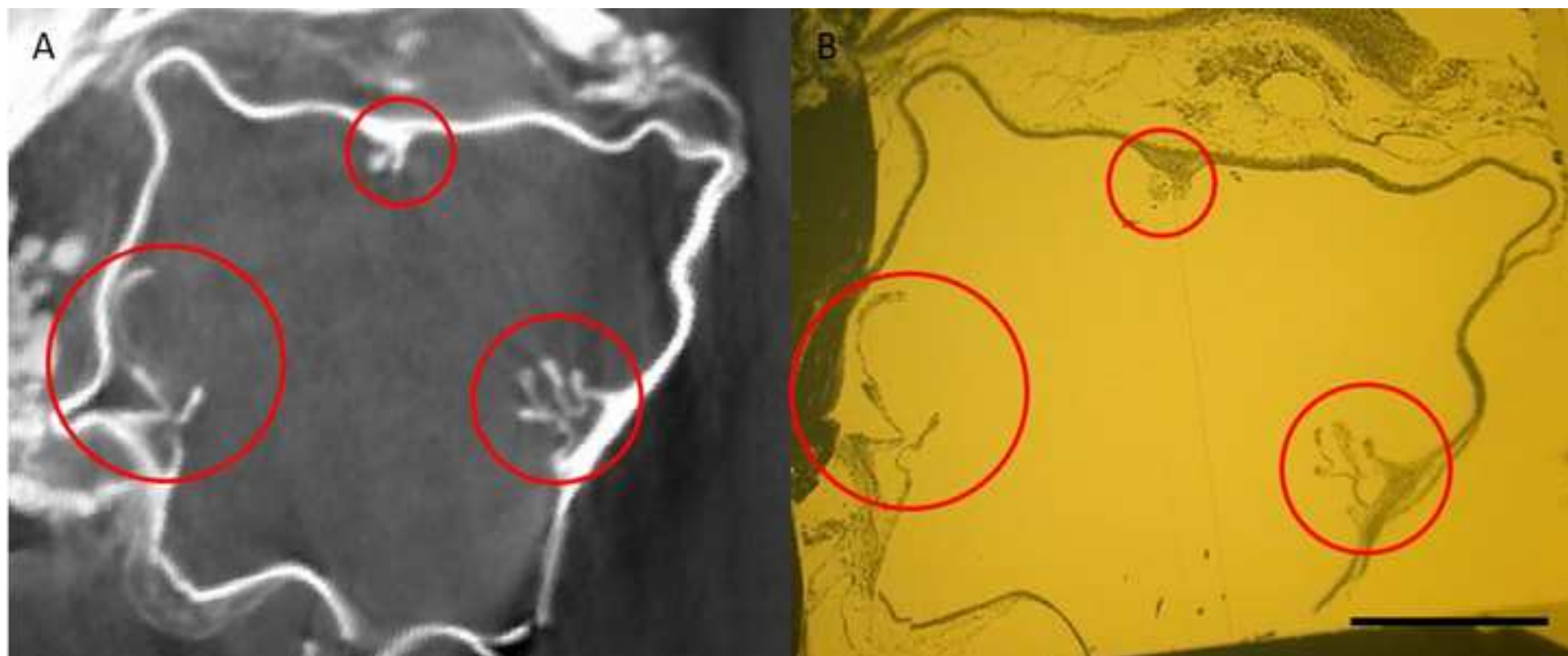
485 valvulogenic, chondrogenic, and osteogenic pathways in mouse models of myxomatous
486 and calcific aortic valve disease. *Journal of Molecular and Cellular Cardiology*. **52** (3), 689–
487 700 (2012).

- 488 4. Jiménez-Altayó, F. et al. Stenosis coexists with compromised α 1-adrenergic contractions
489 in the ascending aorta of a mouse model of Williams-Beuren syndrome. *Scientific Reports*.
490 **10** (1), 889 (2020).
- 491 5. Thacoor, A. Mitral valve prolapse and Marfan syndrome. *Congenital Heart Disease*. **12** (4),
492 430–434 (2017).
- 493 6. McAnulty, P., Dayan, A., Ganderup, N.-C., Hastings, K., Dawson, H. A Comparative
494 Assessment of the Pig, Mouse and Human Genomes. *The Minipig in Biomedical Research*.
495 CRC Press. (2011).
- 496 7. Hinton, R. B., Yutzey, K. E. Heart valve structure and function in development and disease.
497 *Annual Review of Physiology*. **73**, 29–46 (2011).
- 498 8. Hinton, R. B. et al. Extracellular matrix remodeling and organization in developing and
499 diseased aortic valves. *Circulation Research*. **98** (11), 1431–1438 (2006).
- 500 9. Sacks, M. S., Merryman, W. D., Schmidt, D. E., David Merryman, W., Schmidt, D. E. On the
501 biomechanics of heart valve function. *Journal of Biomechanics*. **42** (12), 1804–1824 (2009).
- 502 10. Sacks, M. S., Yoganathan, A. P. Heart valve function: a biomechanical perspective.
503 *Philosophical Transactions of the Royal Society B-Biological Sciences*. **362** (1484), 1369–
504 1391 (2007).
- 505 11. Morales, A. G. et al. Micro-CT scouting for transmission electron microscopy of human
506 tissue specimens. *Journal of Microscopy*. **263** (1), 113–117 (2016).
- 507 12. Sacks, M. S., Smith, D. B., Hiester, E. D. The aortic valve microstructure: Effects of
508 transvalvular pressure. *Journal of Biomedical Materials Research*. **41** (1), 131–141 (1998).
- 509 13. Ayoub, S. et al. Heart valve biomechanics and underlying mechanobiology. *Comprehensive*
510 *Physiology*. **6** (4), 1743–1780 (2016).
- 511 14. Stella, J. A., Liao, J., Sacks, M. S. Time-dependent biaxial mechanical behavior of the aortic
512 heart valve leaflet. *Journal of Biomechanics*. **40** (14), 3169–3177 (2007).
- 513 15. Korn, E. D., Weisman, R. A. I. loss of lipids during preparation of amoebae for electron
514 microscopy. *Biochimica et Biophysica Acta (BBA)/Lipids and Lipid Metabolism*. **116** (2),
515 309–316 (1966).
- 516 16. Tapia, J. C. et al. High-contrast en bloc staining of neuronal tissue for field emission
517 scanning electron microscopy. *Nature Protocols*. **7** (2), 193–206 (2012).
- 518 17. Hinton, R. B. et al. Mouse heart valve structure and function: Echocardiographic and
519 morphometric analyses from the fetus through the aged adult. *American Journal of*
520 *Physiology - Heart and Circulatory Physiology*. **294** (6), H2480–H2488 (2008).
- 521 18. Denk, W., Horstmann, H. Serial block-face scanning electron microscopy to reconstruct
522 three-dimensional tissue nanostructure. *Plos Biology*. **2** (11), 1900–1909 (2004).
- 523 19. Lincoln, J., Florer, J. B., Deutsch, G. H., Wenstrup, R. J., Yutzey, K. E. ColVa1 and ColXla1 are
524 required for myocardial morphogenesis and heart valve development. *Developmental*
525 *Dynamics*. **235** (12), 3295–3305 (2006).
- 526 20. Hamatani, Y. et al. Pathological investigation of congenital bicuspid aortic valve stenosis,
527 compared with atherosclerotic tricuspid aortic valve stenosis and congenital bicuspid
528 aortic valve regurgitation. *PLoS One*. **11** (8) (2016).

Figure 1







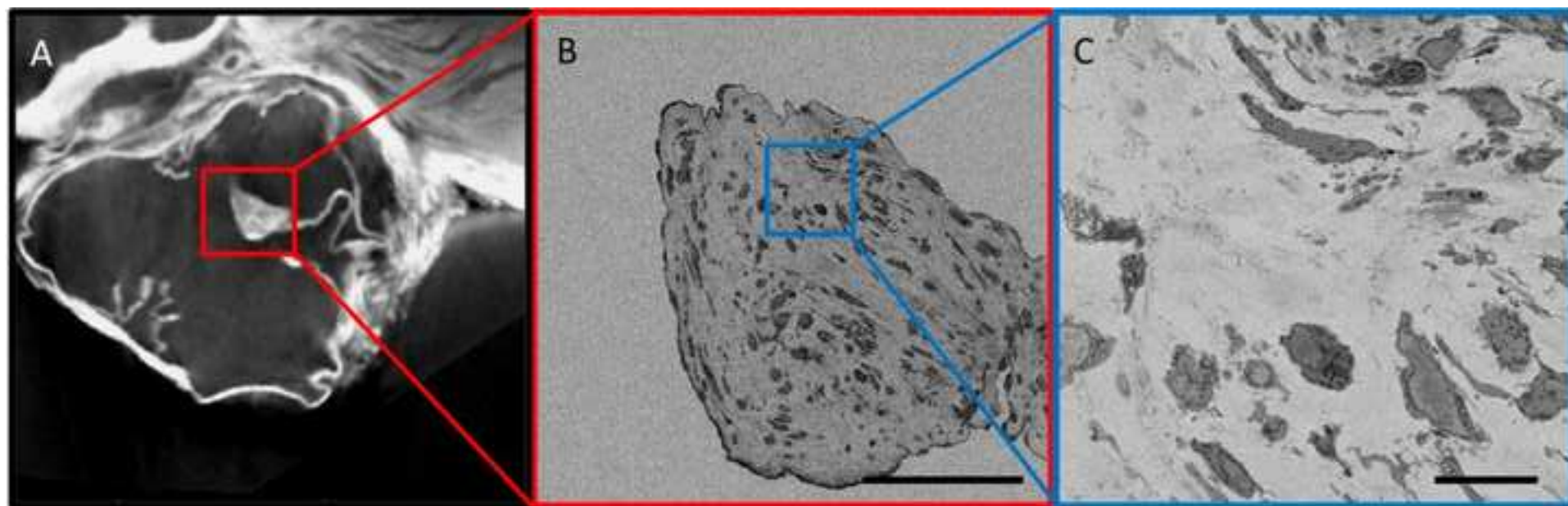
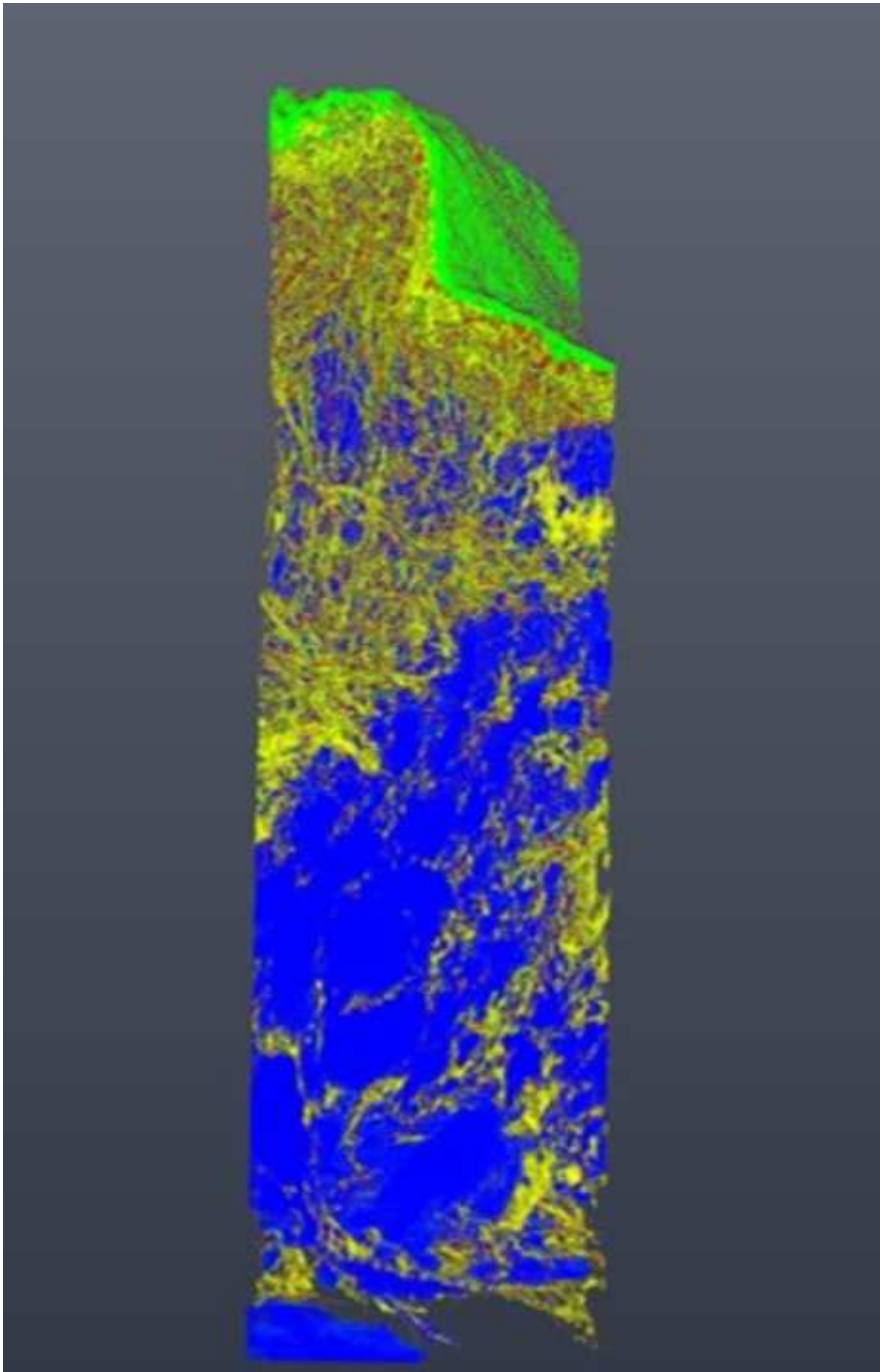
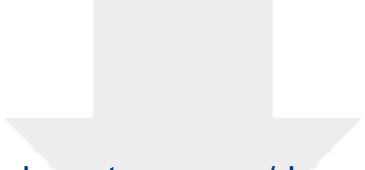


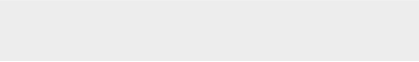
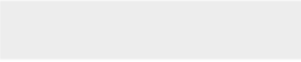
Figure 5

[Click here to access/download;Figure;JoVe Fig 5.jpg](#) 





Click here to access/download
Video or Animated Figure
Media1.mp4



Supplemental
Table S1: Imaging parameters for μ CT

Tube potential	70 kV
Tube current	75 μ A
Focus mode	M
Trajectory	Circular
Projections/Revolution	2880
Mode	3040 x 3040 px
Averaging	1
Exposure time	1.0 s
Sample-to-gun distance	15 mm
Detector-to-gun distance	725 mm
Voxel size	2.9 μ m
Field of view	8.4 x 8.4 x 6.3 mm

Supplimentary
Table S2: Imaging parameters for SBF-SEM

Landing energy	2 - 2.5 kV
Beam current	100 - 400 pA
Working distance	6.5 - 7 mm
Detector	VS-DBS
Dwell time	1 - 2 μ s

Reagent

25% glutaraldehyde (aq)
 0.9% sodium chloride injection
 1 mL syringe
 10 mL syringe
 200 proof ethanol
 22G needle
 3 mL syringe
 3-way stopcock
 4% osmium tetroxide
 4% paraformaldehyde (aq)
 Absorbable hemostat
 Acetone
 Black polyamide monofilament suture, 10-0
 Black polyamide monofilament suture, 6-0
 C57BL/6 mice
 Calcium chloride
 Clamp applying forcep
 Cotton tip applicators
 DPBS
 Dumont #5 forcep
 Dumont #5/45 forceps
 Dumont #7 fine forcep
 Durcupan ACM resin
 Fine scissor
 Heliscan microCT
 Ketamine hydrochloride injection
 L-aspartic acid
 Lead nitrate
 low-vacuum backscatter detector
 Micro-adson forcep
 Millex-GP filter, 0.22 um, PES 33mm, non-sterile
 Non-woven sponges
 Potassium hexacyanoferrate(II) trihydrate
 Potassium hydroxide
 Pressure monitor line
 Saline solution (sterile 0.9% sodium chloride)
 Size 3 BEEM capsule
 Sodium cacodylate trihydrate
 Solibri retractors
 Sputter, carbon and e-beam coater
 Surgical microscope
 Thiocarbohydrazide (TCH)
 Tish needle holder/forcep
 Trimmer
 Uranyl acetate

Company

EMS
 Hospira Inc.
 BD
 BD
 EMS
 BD
 BD
 Smiths Medical ASD, Inc.
 EMS
 EMS
 Ethicon
 EMS
 ARO Surgical instruments Corporation
 ARO Surgical instruments Corporation
 Jackson Laboratories
 Sigma-Aldrich
 FST
 Fisher Scientific
 Gibco
 FST
 FST
 FST
 EMS
 FST
 Thermo Fisher Scientific
 Hospira Inc.
 Sigma-Aldrich
 EMS
 Thermo Fisher Scientific
 FST
 EMD Millipore
 McKesson Corp.
 Sigma-Aldrich
 Sigma-Aldrich
 Smiths Medical ASD, Inc.
 Hospira Inc.
 EMS
 Sigma-Aldrich
 FST
 Leica
 Leica
 EMS
 Micrins
 Wahl
 EMS

Volumescape scanning electron microscope
Xylazine sterile solution

Thermo Fisher Scientific
Akorn Inc.

Catalog Number	Comments/Description
16210	Primary fixative component
NDC 0409-4888-10	
309659	
309604	
15055	
305156	
309657	
MX5311L	Staining component
19150	
157-4-100	Primary fixative component
1961	
10012	Approximately 1 yo
TI38402	
SN-1956	
664	
10043-52-4	
00072-14	
23-400-118	
14190-144	
11251-20	
11251-35	
11274-20	For embedding
14040	
14028-10	Micro-CT
NDC 0409-2053	
56-84-8	Staining component
17900	
VSDBS	SEM backscatter detector
11018-12	
SLGP033NS	Staining component
94442000	
14459-95-1	
1310-58-3	Embedding container
MX562	
NDC 0409-0138-22	Buffer
69910-01	
6131-99-3	Gold coater
17000-04	
EM ACE600	Staining component
M80	
21900	Staining component
MI1540	
9854-500	
22400	Staining component

VOLUMESCOPESEM

Serial Block Face Scanning Electron Microscope

NADA# 139-236

1. The editor has formatted the manuscript to match the journal's style. Please retain and use the attached version for revision.
2. Please address all the comments marked in the manuscript.

Addressed to the best of my ability.

3. Once done please ensure that the highlighted section is in line with the manuscript and fits the 3 page limit including headings and spacings. This will be used for generating scripts for the video.

Highlighted.

4. If you would like to use your own video, please ensure that you have someone in your team record your own interview statements (this will be done after the manuscript is accepted and the script is made). Also, please upload all current videos to the dropbox link provided below (and timestamp with the step number), so our production team can see and ensure that the video is up to our standards. If not, you will be asked to reshoot. To keep things simple, we can film your entire video once the manuscript is accepted and the script is done. This will also ensure better quality. Please let me know how you would like to proceed.

After speaking with the authors I think it is most convenient if JoVE brings in a production team to film the highlighted portion of the manuscript. However, since this only covers the animal dissection, we would like to demonstrate the image correlation between the microCT and SEM imaging using the submitted video. In this case, would the video need to be referenced in the text?

<https://www.dropbox.com/request/qar114oZwQ4gYjbtDW85?oref=e>